

# The constraint of plasma power balance on runaway avoidance

Christopher J. McDevitt

*Nuclear Engineering Program, University of Florida, Gainesville, FL 32611*

Xian-Zhu Tang, Christopher J. Fontes, Prashant Sharma  
*Los Alamos National Laboratory, Los Alamos, NM 87545*

Hyun-Kyung Chung

*Korea Institute of Fusion Energy, 169-148 Gwahak-ro, Yuseong-gu, Daejeon 34133, Korea*

(Dated: October 21, 2022)

In a post-thermal-quench plasma, mitigated or unmitigated, the plasma power balance is mostly between collisional or Ohmic heating and plasma radiative cooling. In a plasma of atomic mixture  $\{n_\alpha\}$  with  $\alpha$  labeling the atomic species, the power balance sets the plasma temperature, ion charge state distribution  $\{n_\alpha^i\}$  with  $i$  the charge number, and through the electron temperature  $T_e$  and ion charge state distribution  $\{n_\alpha^i\}$ , the parallel electric field  $E_\parallel$ . Since the threshold electric field for runaway avalanche growth  $E_{av}$  is also set by the atomic mixture, ion charge state distribution and its derived quantity, the electron density  $n_e$ , the plasma power balance between Ohmic heating and radiative cooling imposes a stringent constraint on the plasma regime for avoiding and minimizing runaways when a fusion-grade tokamak plasma is rapidly terminated.

The fast termination of a fusion-grade plasma in a tokamak reactor is prone to Ohmic-to-runaway current conversion [1], which is made extraordinarily efficient by the avalanche mechanism [2–4] due to the knock-on collisions between primary runaways and background free and bound electrons [5–7]. Such fast shutdowns could be intentional, for safety upon the detection of an inadvertent sub-system fault, for example, or unplanned, as the result of a tokamak disruption. Disruptions can have a variety of causes [8] including such a mundane event as a falling tungsten flake into the plasma. For the relativistic energies characteristic of runaway electrons (RE), their local deposition on the first wall can induce severe surface and sub-surface damage of plasma facing components. A straightforward and perhaps ideal approach to mitigate RE damage is to minimize the runaway population by avoiding the runaway avalanche altogether. This is the so-called runaway electron avoidance problem in a tokamak plasma.

The most troublesome feature of a fast shutdown, as in a tokamak disruption, is the ease for a fusion-grade plasma to rid its thermal energy in comparison with the plasma current. The so-called thermal quench (loss of plasma thermal energy) is often one to two orders of magnitude (if not more) shorter than the current quench (decay of plasma current) [1]. In a post-thermal-quench plasma, mitigated or not, the plasma power balance is mostly between collisional or Ohmic heating and plasma radiation. This is usually the case because the post-thermal-quench plasma temperature is clamped by high-Z impurity radiation to be a very low value, likely in the range of a few electron volts. Radial transport at such low thermal energies is relatively slow, even in the presence of a stochastic magnetic field [9, 10]. The source of high-Z impurities could be divertor/wall materials that are introduced into the plasma through intense plasma-wall interaction during the thermal quench when the bulk of the plasma thermal energy is dumped on the plasma-facing components. In a mitigated thermal quench, high-Z impurities, such as neon or argon, are

deliberately injected into the plasma via pellets or gas jets.

In the standard scenario where the thermal quench is fast and the post-thermal-quench plasma is cold and rich in high-Z impurities, an Ohmic-to-runaway current conversion is inevitable when a finite RE seed and large amount of plasma current is present. This results in the formation of a runaway plateau shortly after the thermal quench. An interesting discovery, from experiments on both DIII-D [11] and JET [12], is that the high-Z impurities can be purged by a massive hydrogen injection in the runaway plateau phase. The resulting, mostly hydrogen plasma can expel the runaway electrons via a large-scale MHD event that stochasticizes the magnetic fields globally. The details of the underlying MHD instabilities vary in DIII-D and JET experiments [13], but the expectation that open field lines lead to rapid runaway loss via parallel streaming is robustly met in both devices. The added benefit is the experimental observation that the runaways are broadly dispersed onto the first wall so no appreciable localized heating is detected. The so-called MHD flush of the runaways after an impurity purge leaves the possibility that the mostly hydrogenic plasma could reheat to sustain an Ohmic current without crossing the avalanche threshold. This is the topic of the current paper.

In a plasma of atomic mix  $\{n_\alpha\}$  with  $\alpha$  labeling the atomic species, the power balance between Ohmic heating and radiative cooling sets the plasma temperature, ion charge state distribution  $\{n_\alpha^i\}$  with  $i$  the charge number, and through the electron temperature  $T_e$ , the ion charge state distribution  $\{n_\alpha^i\}$ , and the parallel electric field  $E_\parallel$ . Since the threshold electric field for runaway avalanche growth  $E_{av}$  is also set by the atomic mixture, charge state distribution and its derived quantity, the electron density  $n_e$ , the plasma power balance between Ohmic heating and radiative cooling imposes a stringent constraint on the plasma regime for avoiding and minimizing runaways when a fusion-grade tokamak plasma is to be terminated either intentionally or unintentionally. Robust

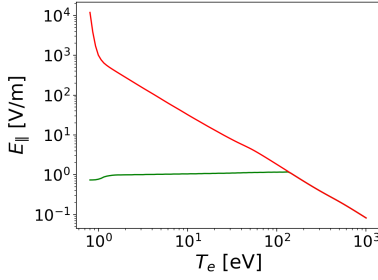


Figure 1. Transition between Ohmic and RE roots. The red curve indicates the parallel electric field on the Ohmic root, whereas the green curve indicates the parallel electric field on the RE root. The temperature at which the curves intersect defines  $T_{av}$ . The deuterium density was taken to be  $n_D = 10^{21} \text{ m}^{-3}$ , the neon density  $n_{Ne} = 10^{19} \text{ m}^{-3}$ , and the current density was taken to be  $j = 2 \text{ MA/m}^2$ .

RE avoidance can be achieved if Ohmic heating is able to offset the radiative and transport losses, and reheat the plasma so the parallel electric field  $E_{\parallel} = \eta j_{\parallel}$  drops below the runaway avalanche threshold  $E_{av}$ . If this could be maintained over the remainder of the current quench, effective runaway “avoidance” would have been achieved. The key question is the critical deuterium density and the fractional neon impurity density below which such a scenario can be triggered. A second question is whether the reheated plasma can be placed in the regime that the Ohmic current quench falls within the known design constraint for the current quench duration, which in the case of ITER has an upper bound of 150 milliseconds (ms) and a lower bound of 50 ms [1, 14].

This Letter lays out the basic physics considerations underlying the answers to both questions explained above, which are of practical importance to a tokamak reactor like ITER. From the plasma power balance between Ohmic heating and radiative cooling, we find that the operational space for plasma reheating and runaway avoidance is highly constrained in terms of the plasma density and the remnant impurity content. This can be illustrated by considering the quasi-steady state parallel electric field as a function of the electron temperature, an example of which is plotted in Fig. 1. First considering the case in which a negligible number of runaway electrons are present, the parallel electric field will be given by  $E_{\parallel} = \eta j_{\parallel}$ , with  $\eta$  the plasma resistivity and  $j_{\parallel}$  the plasma parallel current density [15]. Noting that the plasma resistivity scales as  $\eta \propto 1/T_e^{3/2}$ , the electric field will decrease rapidly as  $T_e$  is increased for a given plasma current density  $j_{\parallel}$ . Once the magnitude of the electric field has dropped below  $E_{av}$ , runaway electron amplification by the avalanche mechanism will no longer be possible. The electron temperature at which this occurs will be referred to as  $T_{av}$ . For temperatures below  $T_{av}$ , two distinct roots of the system are present. This can be motivated by considering an Ohm’s law, modified to account for the presence of runaway electrons, of the form:

$$E_{\parallel} = \eta (j_{\parallel} - j_{RE}).$$

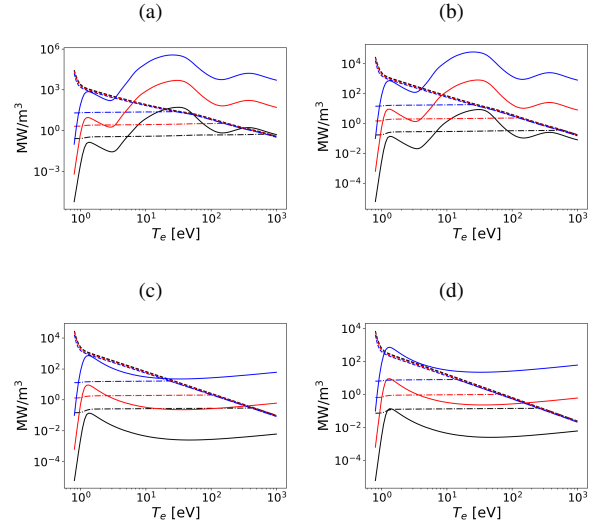


Figure 2. Ohmic heating  $\eta j^2$  (dashed lines) with current carried by background electrons, collisional heating  $\mathbf{E}_{av} \cdot \mathbf{j}$  (dashed-dotted lines) with current carried by runaway electrons and  $E_{av}$  the avalanche threshold field, and radiative cooling rate  $P_{rad}$  (solid lines) are shown as a function of  $T_e$  and for three deuterium densities:  $n_D = 10^{20} \text{ m}^{-3}$  (black),  $n_D = 10^{21} \text{ m}^{-3}$  (red), and  $n_D = 10^{22} \text{ m}^{-3}$  (blue). There are 4 cases shown: (a)  $j = 2 \text{ MA/m}^2$ ,  $n_{Neon}/n_D = 5\%$ ; (b)  $j = 2 \text{ MA/m}^2$ ,  $n_{Neon}/n_D = 1\%$ ; (c)  $j = 2 \text{ MA/m}^2$ ,  $n_{Neon} = 0$ ; (d)  $j = 1 \text{ MA/m}^2$ ,  $n_{Neon} = 0$ .

For  $j_{RE} \ll j_{\parallel}$ , the electric field can again be approximated by  $E_{\parallel} \approx \eta j_{\parallel}$ , which yields the red curve shown in Fig. 1. For  $T_e < T_{av}$  this root can, however, be recognized to be unstable. In particular, since  $E_{\parallel} > E_{av}$  when  $T_e < T_{av}$ , any seed RE population present in the plasma will be amplified by the avalanche mechanism. As a larger fraction of the plasma current is carried by REs, this will cause  $E_{\parallel}$  to drop until  $E_{\parallel} \approx E_{av}$  [4, 16]. This second root, which we will refer to as the RE root, is stable for  $T_e < T_{av}$ , and leads to the formation of a current plateau. Thus, a sufficient condition to avoid RE formation is to maintain  $T_e \gtrsim T_{av}$ . The primary challenge is to identify a solution whereby  $T_e \gtrsim T_{av}$  while simultaneously adhering to the ITER requirement of a current quench timescale in the range of 50-150 ms. [14]

The challenge of simultaneously satisfying these two constraints is made evident in the power balance curves illustrated in Fig. 2. Here, the Ohmic heating rate is plotted along with the radiative cooling rate  $P_{rad}$  as a function of the electron temperature  $T_e$ . The bulk plasma heating can be estimated by multiplying the parallel electric field sketched in Fig. 1 by the plasma current density. For the Ohmic root, this leads to the familiar expression  $P_{\eta} \equiv \eta j_{\parallel}^2$ . For the RE root, this leads to the net energy transferred to the plasma being given by  $P_{RE} = E_{av} j_{\parallel}$ . While a small fraction of this energy will be lost via radiative losses in the channels of synchrotron radiation [17, 18], bremsstrahlung [19], and line emission [20, 21], the majority of this energy will be collisionally transferred to the bulk electrons. Thus, at steady state

the heating of the bulk electrons will be bounded from above by  $P_{RE} = E_{av}j_{\parallel}$  when on the RE root. For given atomic densities of deuterium and neon impurities, the collisional-radiative codes FLYCHK [22] (for D) and ATOMIC [23] (for Ne) are used to compute the charge state distribution and the radiative cooling rate, in the steady-state approximation, as a function of  $T_e$ . The free electron density  $n_e$  is then found from quasineutrality. The charge state distribution is then fed into the avalanche threshold evaluation using the runaway vortex O-X merger model [24], which accounts for the partial screening effect using the collisional friction and pitch angle scattering rates given in Hesslow, et al. [25]. This latter step yields an estimate of the avalanche threshold as a function of the plasma composition. It is interesting to note that at very low  $T_e$ , there is a sizable neutral population and the electron-neutral collisions can contribute significantly to collisional friction [26–28]. This is reflected by the enhanced Ohmic heating at the low  $T_e$  end in Fig. 2, where the Ohmic heating power, after factoring in the electron-neutral collisions, deviates from the  $T_e^{-3/2}$  scaling that is predicted from the Spitzer resistivity.

Recall that a mitigated post-thermal-quench plasma is radiatively clamped to low  $T_e$ , likely in the range of a few eVs, and the purge of neon by massive deuterium injection involves a further cooling of  $T_e$ , so the reheating of the bulk plasma necessarily starts from the very low  $T_e$  end, most likely below the first peak of the radiative cooling rate curve shown in Fig. 2, which is set by deuterium, not the neon impurity. For high enough deuterium density  $n_D$  and at modest plasma current density, Ohmic heating may not be able to overcome this first peak in the radiative cooling curve, and there is no significant reheating of  $T_e$  possible. This is shown by the solid blue curve (radiative cooling) in Fig. 2(d) in comparison with the dotted-dash line (Ohmic heating). It is of interest to note that the deuterium radiative peak, in the case of  $n_D = 10^{22} \text{ m}^{-3}$ , is very close to the  $P_{\eta}$  curve in Fig. 2(a,b). If  $j_{\parallel}$  is dropped from 2 MA/m<sup>2</sup> to 1 MA/m<sup>2</sup> in these two cases,  $P_{\eta}$  will also cross the deuterium radiative cooling peak. For the deuterium radiation peak to safely stay below  $P_{\eta}$ , the deuterium density  $n_D$  must be lower, by an amount that scales with  $j_{\parallel}^{1/2}$ . For discharges that satisfy this constraint, the mostly hydrogenic plasma will be reheated above the deuterium peak, which is around  $T_e = 1.2 \text{ eV}$ . This deuterium density constraint is a necessary, but generally not sufficient condition, for the plasma to be reheated enough to avoid runaways. The complication comes from the presence of remnant impurities.

In Fig. 2(a,b), one can see that the presence of neon impurities, as small as 1-5% in fractional number density, introduces a second radiative cooling peak in the range of  $T_e \approx 30 \text{ eV}$ . The first crossing point between the radiative cooling ( $P_{rad}$ ) curve and the Ohmic heating ( $P_{\eta}$ ) curve marks the critical electron temperature  $T_{reheat}$  that the reheating of the plasma will be bounded from above. From Fig. 2(a), we find that with high enough  $n_{neon}$  (5% for this case),  $T_{reheat}$  is in the range of a few eV to 30 eV. This suggests an in-range Ohmic current quench time, but avalanche is unavoidable because

$T_{reheat} < T_{av}$  for all three densities.

To further quantify this concept, we recall that the parallel electric field at  $T_{reheat}$  for an Ohmic plasma (i.e. the plasma current is purely Ohmic), is simply  $E_{reheat} \equiv E_{\parallel}(\eta) = \eta j_{\parallel}$ . We can plot the  $P_{RE} = E_{av}j_{\parallel}$  in the same plot, and the ratio of  $P_{\eta}(T_{reheat}) = \eta(T_{reheat})j_{\parallel}^2$  and  $P_{RE}$  is just the ratio of  $E_{reheat}$  and  $E_{av}$ . Equivalently, we can cast the ratio of  $E_{reheat}$  and  $E_{av}$  in terms of the  $T_{av}/T_{reheat}$ , with  $T_{av}$  the intercept of the runaway heating curve  $P_{RE}$  and the Ohmic heating curve  $P_{\eta}$ . Since  $E_{\parallel}(\eta) = \eta j_{\parallel} \propto Z_{eff}/T_e^{3/2}$  with  $Z_{eff}$  the effective ion charge of the plasma, one finds

$$\frac{E_{reheat}}{E_{av}} = \frac{Z_{eff}(T_{reheat})}{Z_{eff}(T_{av})} \left( \frac{T_{av}}{T_{reheat}} \right)^{3/2}. \quad (1)$$

Figure 2(b) reveals that even with five times lower neon densities,  $n_{neon} = 10^{20} \text{ m}^{-3}$  (solid blue line) and  $n_{neon} = 10^{19} \text{ m}^{-3}$  (solid red line), which correspond to fractional number density of 1% for neon impurities in a deuterium plasma,  $E_{reheat}/E_{av} \geq 10$ . For such a large parallel electric field, we anticipate robust runaway current reconstitution via the avalanche mechanism.

To safely avoid runaways,  $E_{\parallel} = \eta(T_e)j_{\parallel}$  should stay below  $E_{av}$ , which corresponds to  $T_{av} < T_{reheat}$ . From Fig. 2(a,b), we find that only the case of lowest  $n_D$  ( $10^{20} \text{ m}^{-3}$ ) and impurity content ( $n_{Neon}/n_D = 1\%$ ) satisfies this requirement. And when it does, the plasma actually recovers from the disruption by reaching electron temperatures in excess of one keV. This could be a favorable outcome in a tokamak that offers sufficiently fast positional control to avoid vertical displacement events (VDEs). In an ITER-like reactor, reheating of the plasma with less plasma current simply implies a hot VDE due to the long wall time of the vacuum vessel.

If the goal is to terminate the plasma for a shut down of the reactor, the more desirable scenario lies with much reduced impurity radiation, but high deuterium density to prevent the plasma from achieving electron temperatures in excess of a keV. The limiting case is  $n_{neon} = 0$  is shown in Fig. 2(c,d). One can see that  $n_D = 10^{21} \text{ m}^{-3}$  (solid red curve) is high enough to force  $T_{av} < T_{reheat}$ , so the Ohmic electric field stays below the avalanche threshold. The choice of even higher deuterium densities, for example, the blue curves in Fig. 2(c) for  $n_D = 10^{22} \text{ m}^{-3}$ , offers the intriguing possibility of a lower  $T_{reheat}$  with an Ohmic electric field that is marginally above the avalanche threshold electric field at  $j = 2 \text{ MA/m}^2$ . The  $T_{reheat}$  is more consistent with a current quench duration of 100 ms envisioned for ITER, which is in the range of 10-15 eV or so for a deuterium plasma. This promising prospect is complicated by the fact that as the plasma current density drops from 2 MA/m<sup>2</sup> to 1 MA/m<sup>2</sup>, the reduction in Ohmic heating power would lead to a radiatively clamped  $T_e$  below the deuterium peak around 1.2 eV in a plasma of  $n_D = 10^{22} \text{ m}^{-3}$ , resulting in an Ohmic electric field significantly above avalanche threshold, see Fig. 2(d). To avoid the avalanche growth of runaways during the current quench, one thus relies on (1) the current-carrying plasma

shrinking in size as  $I_p$  decays but maintaining comparable  $j_{\parallel}$ , or (2) a way to dynamically reduce the plasma particle density as  $I_p$  and  $j_{\parallel}$  decay in time.

A number of observations can be made here on both (1) and (2). For (1), it is indeed the case that as the toroidal plasma current  $I_p$  decreases, the current-carrying plasma column does shrink. The resulting change in  $j_{\parallel}$  is modest, at most by a factor of two in an ITER-like plasma initially with 15 MA of plasma current. In a goldilocks situation with  $T_e$  fixed, a factor of 2 drop in  $j_{\parallel}$  produces a factor of 4 decrease in  $P_{\eta}$ . Since the deuterium radiative cooling rate scales with the product of the ion and electron densities, which is approximately equal in the  $T_e \geq 10$  eV range, in order to balance the reduced Ohmic heating rate, the  $n_D$  would have to be reduced by a factor of 2 as well. In practice, the more likely scenario is that the reduced Ohmic heating due to a lower  $j_{\parallel}$  would lower  $T_e$ , boosting the deuterium radiative power loss rate in the temperature range of  $T_e = 10 - 30$  eV. This would further aggravate the need to further reduce  $n_D$ . Reduction of  $n_D$  in the temperature range of  $T_e \approx 10 - 20$  eV can only be achieved via plasma transport, which can be sustained in a discharge if particle pumping at the chamber boundary is maintained in a post-thermal-quench plasma.

The potential remedy to possibly impede a drop of  $T_e$  with a decreasing  $j_{\parallel}$  lies with physical mechanisms that can reduce plasma cooling with a decreasing  $T_e$ . In the targeted range of  $T_e \approx 10 - 20$  eV, neon radiation intensity rapidly decreases with a decreasing  $T_e$ . This suggests the mitigating role of neon impurities. By contrasting the radiation intensity of deuterium and neon around  $T_e = 20$  eV at fixed  $n_e = 10^{22}/\text{m}^3$ , one finds that a fractional number density of  $10^{-5}$  for the neon impurity would have the neon impurity radiative cooling rate twice that of the bulk deuterium plasma. Along the same line, if the neon fractional number density is  $10^{-6}$ , the neon radiation would be 1/5 of the deuterium's, and it would have a negligible off-setting effect in reducing the cooling rate as  $T_e$  drops.

The case studies shown so far clarify the basic physics considerations and the resulting constraints on the plasma regime for avoiding runaway avalanche in a post-thermal-quench plasma. Next we perform a more comprehensive scan to demarcate the preferred operational regime in terms of  $(n_D, n_{neon})$ . Two derived quantities will be used to characterize the operational regime. These are  $\mathcal{E} \equiv E_{reheat}/E_{av} - 1$  and  $T_{reheat}$ , all of which were previously explained in the text and computed in Fig. 2. The result of this calculation is shown in Fig. 3 for two different current densities. Two temperature contours are also plotted, where to remain within the current decay time targeted by ITER the electron temperature should remain roughly in the range of  $T_e \approx 10 - 20$  eV. Considering first a high current density case [see Fig. 3(a)] with  $j_{\parallel} = 2 \text{ MA/m}^{-2}$ , it is evident that the system will remain well above the avalanche threshold unless a near complete purge of the neon is present. Furthermore, for low to modest deuterium densities ( $n_D \lesssim 2 \times 10^{15} \text{ cm}^{-3}$ ) the regions below the avalanche threshold (white contour in Fig. 3) coincide with electron temperature in excess of 100 eV,

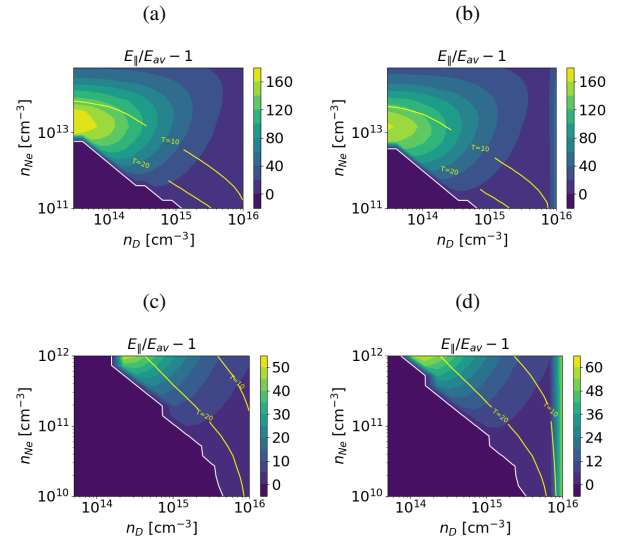


Figure 3. Comparison of the parallel electric field with the avalanche threshold. Panels (a) and (c) are for 2 MA/m<sup>2</sup> and panels (b) and (d) are for 1.5 MA/m<sup>2</sup>. The yellow contours indicate temperature, whereas the white contour is for  $E_{\parallel}/E_{av} - 1 = 0$ .

implying that these cases would have exceptionally long current decay times. At higher deuterium density a solution near the avalanche threshold with a temperature in the range of  $T_e \approx 10 - 20$  eV is present though it requires a near complete purge of the neon. At a modestly lower current density of  $j_{\parallel} = 1.5 \text{ MA/m}^{-2}$  (see Fig. 3(b)), the plasma recombines at the highest deuterium density considered thus leading to a region with  $E_{\parallel}/E_{av} \gg 1$ . This has the effect of shifting the region with  $E_{\parallel}/E_{av} \sim 1$  to lower deuterium densities. Hence, the target deuterium density will depend on the local current density of the plasma. Focusing on the very low neon density regime [Figs. 3(b) and (d)], it is evident that even at very low neon densities, there is no solution below the avalanche threshold with an electron temperature less than 20 eV. It is, however, apparent that a solution with the electric field within a factor of two of the avalanche threshold is present at high deuterium density. Although this cannot avoid the runaway growth of runaway electrons, it does lead to higher poloidal flux consumption in growing the runaway population, which has the favorable effect of reducing the plasma current after runaway reconstitution.

In conclusion, the plasma power balance in a post-thermal-quench plasma places a rigorous constraint on the plasma regime in which runaways can be avoided or minimized. Specifically, unless a current quench duration of greater than 150 ms can be tolerated, there does not appear to be a  $(n_D, n_{Neon})$  regime in which runaway avalanche can be completely avoided. Within the known ITER constraint for current quench duration the high  $n_D$  but negligibly low  $n_{Neon}$  regime can deliver the desired current quench time while minimizing the runaway current, by reaching an Ohmic parallel electric field that is above, but close to, the avalanche threshold elec-

tric field.

We thank the U.S. Department of Energy Office of Fusion Energy Sciences and Office of Advanced Scientific Computing Research for support under the Tokamak Disruption Simulation (TDS) Scientific Discovery through Advanced Computing (SciDAC) project, and the Base Theory Program, both at Los Alamos National Laboratory (LANL) under contract No. 89233218CNA000001. This research used resources of the National Energy Research Scientific Computing Center (NERSC), a U.S. Department of Energy Office of Science User Facility operated under Contract No. DE-AC02-05CH11231 and the Los Alamos National Laboratory Institutional Computing Program, which is supported by the U.S. Department of Energy National Nuclear Security Administration under Contract No. 89233218CNA000001.

- 
- [1] T. Hender, J. Wesley, J. Bialek, A. Bondeson, A. Boozer, R. Buttery, A. Garofalo, T. Goodman, R. Granetz, Y. Gribov, et al., *Nuclear Fusion* **47**, S128 (2007), URL <http://stacks.iop.org/0029-5515/47/i=6/a=S03>.
- [2] I. SOKOLOV, *JETP Letters* **29**, 218 (1979).
- [3] R. Jayakumar, H. Fleischmann, and S. Zweben, *Physics Letters A* **172**, 447 (1993).
- [4] M. Rosenbluth and S. Putvinski, *Nuclear Fusion* **37**, 1355 (1997).
- [5] J. Martín-Solís, A. Loarte, and M. Lehnen, *Nuclear Fusion* **57**, 066025 (2017).
- [6] L. Hesslow, O. Embréus, O. Vallhagen, and T. Fülöp, *Nuclear Fusion* **59**, 084004 (2019).
- [7] C. J. McDevitt, Z. Guo, and X. Z. Tang, *Plasma Physics and Controlled Fusion* **61**, 054008 (2019).
- [8] P. de Vries, M. Johnson, B. Alper, P. Buratti, T. Hender, H. Koslowski, V. Riccardo, and J.-E. Contributors, *Nuclear Fusion* **51**, 053018 (2011), URL <http://stacks.iop.org/0029-5515/51/i=5/a=053018>.
- [9] D. Ward and J. Wesson, *Nuclear fusion* **32**, 1117 (1992).
- [10] B. N. Breizman, P. Aleynikov, E. M. Hollmann, and M. Lehnen, *Nuclear Fusion* **59**, 083001 (2019).
- [11] C. Paz-Soldan, C. Reux, K. Aleynikova, P. Aleynikov, V. Bandaru, M. Beidler, N. Eidietis, Y. Liu, C. Liu, A. Lvovskiy, et al., *Nuclear Fusion* **61**, 116058 (2021).
- [12] C. Reux, C. Paz-Soldan, P. Aleynikov, V. Bandaru, O. Ficker, S. Silburn, M. Hoelzl, S. Jachmich, N. Eidietis, M. Lehnen, et al., *Physical Review Letters* **126**, 175001 (2021).
- [13] V. Bandaru, M. Hoelzl, C. Reux, O. Ficker, S. Silburn, M. Lehnen, N. Eidietis, J. Contributors, J. Team, et al., *Plasma Physics and Controlled Fusion* **63**, 035024 (2021).
- [14] E. M. Hollmann, P. B. Aleynikov, T. Fülöp, D. A. Humphreys, V. A. Izzo, M. Lehnen, V. E. Lukash, G. Papp, G. Pautasso, F. Saint-Laurent, et al., *Physics of Plasmas* **22**, 021802 (2015), <https://doi.org/10.1063/1.4901251>, URL <https://doi.org/10.1063/1.4901251>.
- [15] A post-thermal-quench plasma has lost most of its thermal energy and hence pressure, so force-free is a good approximation and  $\mathbf{j} \approx j_{\parallel} \mathbf{B}/B$ .
- [16] B. N. Breizman, *Nuclear Fusion* **54**, 072002 (2014).
- [17] J. Martín-Solís, R. Sánchez, and B. Esposito, *Physics of Plasmas* **7**, 3814 (2000).
- [18] Z. Guo, C. J. McDevitt, and X.-Z. Tang, *Plasma Physics and Controlled Fusion* **59**, 044003 (2017).
- [19] O. Embréus, A. Stahl, and T. Fülöp, *New Journal of Physics* **18**, 093023 (2016), URL <https://doi.org/10.1088/1367-2630/18/9/093023>.
- [20] N. A. Garland, H.-K. Chung, C. J. Fontes, M. C. Zammit, J. Colgan, T. Elder, C. J. McDevitt, T. M. Wildey, and X.-Z. Tang, *Physics of Plasmas* **27**, 040702 (2020), <https://doi.org/10.1063/5.0003638>, URL <https://doi.org/10.1063/5.0003638>.
- [21] N. A. Garland, H.-K. Chung, M. C. Zammit, C. J. McDevitt, J. Colgan, C. J. Fontes, and X.-Z. Tang, *Physics of Plasmas* **29**, 012504 (2022), <https://doi.org/10.1063/5.0071996>, URL <https://doi.org/10.1063/5.0071996>.
- [22] H.-K. Chung, M. Chen, W. Morgan, Y. Ralchenko, and R. Lee, *High energy density physics* **1**, 3 (2005).
- [23] C. J. Fontes, H. L. Zhang, J. A. Jr, R. E. H. Clark, D. P. Kilcrease, J. Colgan, R. T. Cunningham, P. Hakel, N. H. Magee, and M. E. Sherrill, *Journal of Physics B: Atomic, Molecular and Optical Physics* **48**, 144014 (2015), URL <https://doi.org/10.1088/0953-4075/48/14/144014>.
- [24] C. J. McDevitt, Z. Guo, and X.-Z. Tang, *Plasma Physics and Controlled Fusion* **60**, 024004 (2018).
- [25] L. Hesslow, O. Embréus, A. Stahl, T. C. DuBois, G. Papp, S. L. Newton, and T. Fülöp, *Phys. Rev. Lett.* **118**, 255001 (2017), URL <https://link.aps.org/doi/10.1103/PhysRevLett.118.255001>.
- [26] L. Frost, *Journal of applied physics* **32**, 2029 (1961).
- [27] S. Schweitzer and M. Mitchner, *AIAA Journal* **4**, 1012 (1966).
- [28] V. Zhdanov, *Plasma Physics and Controlled Fusion* **44**, 2283 (2002).